

# Analysis and Experiments of a $TM_{010}$ Mode Cylindrical Cavity to Measure Accurate Complex Permittivity of Liquid

Hirokazu KAWABATA<sup>†a)</sup>, Hiroshi TANPO<sup>†</sup>, Members, and Yoshio KOBAYASHI<sup>†</sup>, Fellow

**SUMMARY** A rigorous analysis for a  $TM_{010}$  mode cylindrical cavity with insertion holes is presented on the basis of the Ritz-Galerkin method to realize accurate measurements of the complex permittivity of liquid. The effects of sample insertion holes, a dielectric tube, and air-gaps between a dielectric tube and sample insertion holes are taken into account in this analysis. The validity of this method is verified from measured results of some kinds of liquid.

**key words:** complex permittivity, cylindrical cavity, liquid, Ritz-Galerkin method

## 1. Introduction

A cavity perturbation method has been commonly used [1]–[3] as a simple method for determining the complex permittivity of dielectric rods [4], [5] and liquids [6]–[8]. It is well known in this method that the measurement accuracy is limited because of the influence of sample insertion holes and the calculation error included intrinsically in the perturbation formulas. So far, the analysis of the  $TM_{010}$  mode cylindrical cavity with insertion holes has been performed approximately, so that effects of insertion holes have not been estimated sufficiently [4]–[8]. The authors have presented a rigorous analysis on the basis of the Ritz-Galerkin method for a cavity with insertion holes [9], [10]. Using this analysis, we can obtain the accurate complex permittivity of dielectric rods and liquids. This analysis is valid to the samples with large diameter and high permittivity, but it needs a tedious calculation by computer. To improve the tedious treatment, we presented the accurate and easy-to-treatment measurement by using the charts of relative errors calculated by the rigorous analysis [9], [11].

In this paper, a new measurement method is proposed to measure complex permittivity of liquid more precisely on the basis of the rigorous electromagnetic analysis by the Ritz-Galerkin method. In this analysis, the effects of insertion holes, a dielectric tube, and air-gaps between a dielectric tube and sample insertion holes are taken into account. Some kinds of liquid were measured by this method to verify the usefulness.

## 2. Analysis of the $TM_{010}$ Mode of a Cavity with a Dielectric Tube and Sample Insertion Holes

The configuration of a  $TM_{0mp}$  mode cylindrical cavity to be

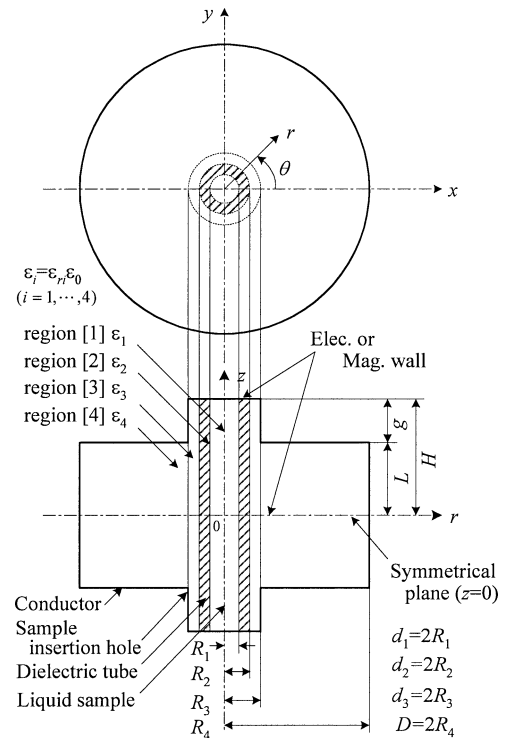


**Fig. 1** Configuration of a  $TM_{0mp}$  mode cylindrical cavity with a dielectric tube and a liquid sample.

analyzed is shown in Fig. 1. The cavity has diameter  $D=2R_4$  and height  $2L$ . Sample insertion holes oriented coaxially have diameter  $d_3=2R_3$  and depth  $g(=H-L)$ , which constitute a cutoff  $TM_{01}$  mode cylindrical waveguide. A dielectric tube, which is used to guide a liquid sample into the cavity, has inner diameter  $d_1=2R_1$ , outer diameter  $d_2=2R_2$  and length  $2H$ . The space in the cavity is divided into four regions  $i$  having the permittivity  $\epsilon_i$ , where  $i=1,2,3$  and 4.

At first, we derive the characteristic equation to obtain the relative permittivity of liquid from a measured frequency  $f_0$ . According to the structural symmetry, the electric or magnetic wall condition is assumed at  $z=0$  and only a half region  $0 < z < H$  is considered. The electric or magnetic wall condition is also assumed at  $z=H$ . A series of higher order modes are taken in each region into account. Imposing the continuity of tangential field components  $E_{zi}$  and  $H_{\theta i}$  at  $r=R_1, R_2$  and  $R_3$  and applying the Ritz-Galerkin method to the integral equation, we obtain the characteristic equation of the  $TM_{0mp}$  mode as follows:

Manuscript received August 29, 2003.

<sup>†</sup>The authors are with the Faculty of Engineering, Saitama University, Saitama-shi, 388-8570 Japan.

<sup>a)</sup> E-mail: kawabata@reso.ees.saitama-u.ac.jp

$$\det X(f_0; \varepsilon_1, \dots, \varepsilon_4, R_1, \dots, R_4, L, H) = 0 \quad (1)$$

where the derivation of Eq. (1) is given in Appendix A. Equation (1) is used to obtain  $\varepsilon_i$ ,  $R_4$  and  $L$  from measured  $f_0$ , as described in Sect. 4.

Then, we discuss the quality factors of a cavity. The field components in each region  $E_{ri}$ ,  $E_{zi}$  and  $H_{\theta i}$  can be calculated by using the solution of Eq. (1) and the expansion coefficients given in Appendix B. The unloaded  $Q$  of the cavity  $Q_u$  is given by

$$Q_u = \omega_0 \frac{1}{P_d + P_c} \sum_{i=1}^4 W_i^e = \left\{ \frac{1}{Q_d} + \frac{1}{Q_c} \right\}^{-1} \quad (2)$$

$$Q_d = \omega_0 \frac{\sum_{i=1}^4 W_i^e}{\sum_{i=1}^4 P_{di}}, \quad Q_c = \omega_0 \frac{\sum_{i=1}^4 W_i^e}{\sum_{i=1}^4 P_{ci}} \quad (3)$$

where  $Q_d$  and  $Q_c$  are the quality factors due to the dielectric loss  $P_d$  and the conductor loss  $P_c$ , respectively. The electric stored energy  $W_i^e$ ,  $P_{di}$  and  $P_{ci}$  in the region  $i$  are given by

$$W_i^e = \frac{1}{2} \varepsilon_i \int_{V_i} (|E_{ri}|^2 + |E_{zi}|^2) dv \quad (4)$$

$$P_{di} = \omega_0 \tan \delta_{ri} W_i^e \quad (5)$$

$$P_{ci} = \frac{1}{2} R_s \int_{S_i} |H_{\theta i}|^2 ds \quad (6)$$

$$\omega_0 = 2\pi f_0, \quad \varepsilon_i = \varepsilon_{ri} \varepsilon_0, \quad \sigma = \sigma_r \sigma_0 \quad (7)$$

$$\sigma_0 = 58 \times 10^6 \text{ (S/m)}, \quad R_s = \sqrt{\frac{\omega_0 \mu_0}{2\sigma}} \quad (8)$$

where  $\sigma$  is the conductivity,  $\sigma_r$  is the relative conductivity of the cavity and  $R_s$  is the surface resistance. As the regions 3 and 4 are the air regions, we put  $\varepsilon_{r3} = \varepsilon_{r4} = 1$  and  $\tan \delta_{r3} = \tan \delta_{r4} = 0$ . From Eqs. (2)–(8),  $\tan \delta_{r1}$  of region 1 is expressed by the following equation:

$$\tan \delta_{r1} = \frac{A}{Q_u} - BR_s - w_2 \tan \delta_{r2} \quad (9)$$

where

$$A = 1 + \sum_{i=2}^4 w_i, \quad B = \frac{1}{\omega_0 R_s} \sum_{i=1}^4 \frac{P_{ci}}{W_i^e}, \quad w_i = \frac{W_i^e}{W_1^e}. \quad (10)$$

### 3. Numerical Results

On the basis of the analysis described in the previous section, a program was developed to calculate  $f_0$  and  $Q$  factors. Numerical calculations were performed for a copper cavity structure used in our experiments. The cavity has  $D=115.172$  mm,  $2L=49.998$  mm,  $g = H - L=10$  mm,  $2R_3=3$  mm and  $\sigma_r=0.790$  [9]. A dielectric tube has  $2R_1=1.062$  mm,  $2R_2=2.077$  mm and  $\varepsilon_{r2}=2.059$  [10]. The

measurements of these parameters will be described in the next section.

The convergence of  $\varepsilon_{r1}$  for pure water was calculated as a function of the numbers of higher order modes  $N$  when  $f_0=1967.331$  MHz and  $\varepsilon_{r2}=2.059$ . The result is shown in Fig. 2(a). It is found that  $N > 100$  is sufficient to obtain an accuracy of four significant figures. The convergences of  $\varepsilon_{r2}$  for a PTFE tube and  $\varepsilon_{r1}$  for pure water were calculated as a function of the depth of insertion holes  $g$ . These results

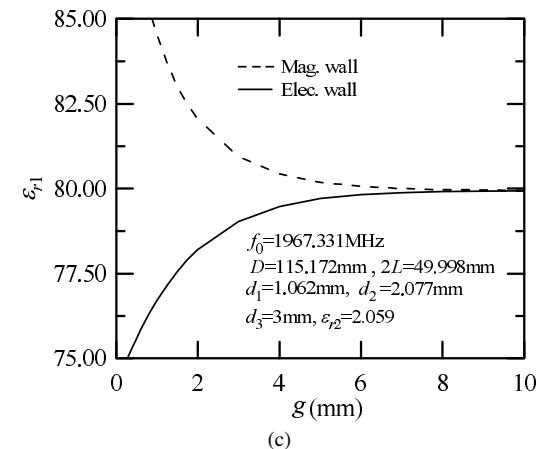
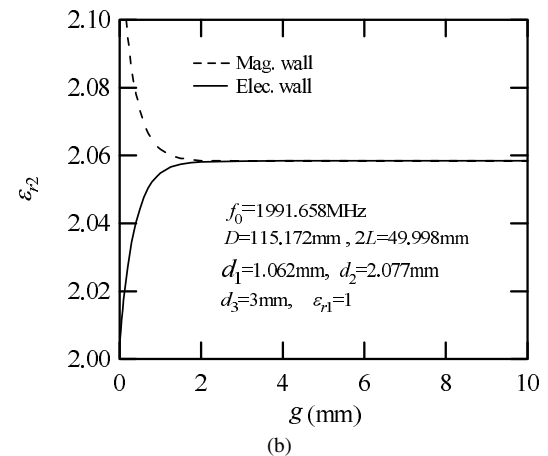
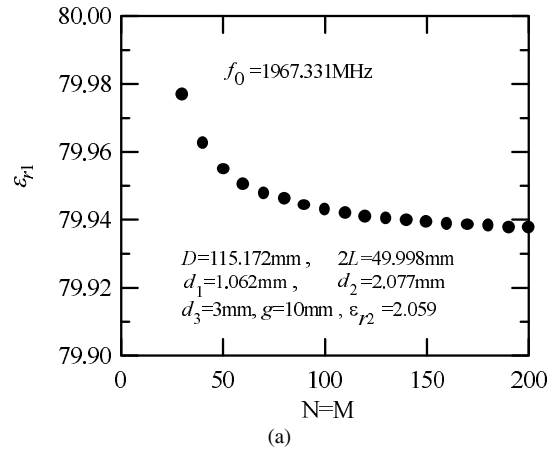


**Fig. 2** Convergences of  $\varepsilon_r$ . (a) as a function of the numbers of higher order modes  $N$ . (b) and (c) as a function of the depth of insertion holes  $g$ .

are shown in Figs. 2(b) and (c), respectively, where the solid and dashed lines are for the electric and magnetic wall conditions at  $z = H$ , respectively. It is seen that  $\epsilon_r$  approaches the constant values when  $g > 2$  mm for  $\epsilon_{r2}$  and  $g > 7$  mm for  $\epsilon_{r1}$  because the fields in the insertion hole regions decay rapidly with  $g$ . Thus,  $H = L + g$  should be determined so as to satisfy  $g > 7$  mm.

## 4. Measured Results

### 4.1 Cavity Parameters

The cavity parameters such as  $D = 2R_4$ ,  $2L$  and  $\sigma_r$  are determined from measured results for the empty cavity (described above) by using Eqs. (1), (7), (8) and (9) with  $\epsilon_{ri}=1$  and  $\tan \delta_i=0$ , where  $i=1$  to 4.  $D$  is obtained from  $f_0$  measured for the  $TM_{010}$  mode.  $2L$  is determined from the  $D$  value and the resonant frequency  $f_2$  measured for the  $TM_{011}$  mode. The accurate values of  $D$  and  $2L$  are obtained by repeating these procedures.  $\sigma_r$  is obtained from  $Q_{u0}$  measured for the  $TM_{010}$  mode as follows [10]:

**Table 1** Measured results of a PTFE tube. (for  $TM_{010}$  at 25°C)

$f_0$ (MHz)	$Q_{u0}$	$\epsilon_{r2}$	$\tan \delta_{r2} (\times 10^{-4})$
1991.658 $\pm 0.003$	15890 $\pm 50$	2.059 $\pm 0.021$	4.0 $\pm 2.1$

$$d_1=1.062\text{mm}, d_2=2.077\text{mm}$$

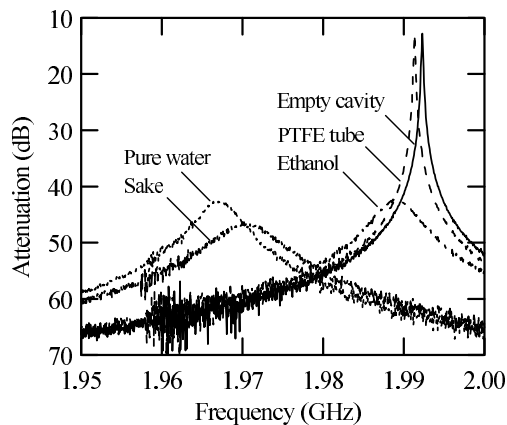


**Fig. 3** Frequency responses of a cavity with liquid samples.

$$\sigma_r = \frac{\omega_0 \mu_0}{2\sigma_0} \left( \frac{B}{A} Q_{u0} \right)^2. \quad (11)$$

The measured result is given in the previous section.

### 4.2 Complex Permittivity of Dielectric Tube

An outer size of the dielectric tube is measured by a micrometer and an inner size is determined from the difference between the tube weight measured with and without water as the relative weight is 0.99707 at 25°C [12]. The complex permittivity of the dielectric tube is obtained from  $f_0$  and  $Q_{u0}$  measured for the  $TM_{010}$  mode of a cavity with the dielectric tube without a liquid sample.  $\epsilon_{r2}$  is obtained from  $f_0$  by using Eq. (1) with  $\epsilon_{r1}=1$ .  $\tan \delta_{r2}$  is determined from  $Q_{u0}$  by using Eq. (9) with  $\tan \delta_{r1}=0$ . These results are shown in Table 1 [10].

### 4.3 Complex Permittivity of Liquids

The measurements of liquid samples filled in the tube were performed after the measurements for the cavity and the dielectric tube. The frequency responses of a cavity with pure water, Japanese sake (water including 14–15% alcohol) and ethanol are shown in Fig. 3, compared with one for the empty cavity. The complex permittivity measured for these liquids are shown in Table 2 and compared with the values calculated by the perturbation method [11]. From Table 2, it is found that the relative errors are approximately within 2.2% for  $\epsilon_p$  and 1.6% for  $\tan \delta_p$ . These errors are caused by the effects of insertion holes, dielectric tube and air-gaps, which are taken into account in the rigorous analysis.

## 5. Conclusions

A new measurement method of the complex permittivity of liquid was proposed on the basis of the rigorous analysis by the Ritz-Galerkin method. Cavity parameters and complex permittivity of a dielectric tube were accurately measured by using this analysis. The measurements of the complex permittivity of liquids were performed to verify the validity and usefulness of this method.

## Acknowledgments

The authors would like to thank Prof. Z. Ma for his helpful

**Table 2** Measured results of some kinds of liquid. (for  $TM_{010}$  with PTFE tube at 25°C)

Material	$f_1$ (MHz)	$Q_{u1}$	The present analysis		Perturbation		Relative error (%)	
			$\epsilon_{r1}$	$\tan \delta_{r1} (\times 10^{-2})$	$\epsilon_p$	$\tan \delta_p (\times 10^{-2})$	$\Delta\epsilon/\epsilon_p$	$\Delta\tan \delta/\tan \delta_p$
Pure water	1967.331 $\pm 0.038$	430 $\pm 10$	79.9 $\pm 0.8$	8.9 $\pm 0.2$	79.4 $\pm 0.8$	9.0 $\pm 0.2$	-0.69	1.6
Japanese Sake (Water including Alcohol)	1970.360 $\pm 0.031$	290 $\pm 10$	70.2 $\pm 0.7$	15.2 $\pm 0.6$	69.5 $\pm 0.7$	15.4 $\pm 0.3$	-1.04	1.3
Ethanol (99.5%)	1989.387 $\pm 0.061$	440 $\pm 20$	8.42 $\pm 0.27$	85.4 $\pm 3.9$	8.24 $\pm 0.22$	85.0 $\pm 2.4$	-2.21	-0.4

discussions.

## References

- [1] N. Ogasawara, "On the measurement of  $\epsilon$  and  $\mu$  by means of the perturbation of cavity resonators," J. IEE Japan, vol.74, no.795, pp.1486–1492, Dec. 1954.
- [2] E. Schanda, "Die Bestimmung von Dielektrizitätskonstante und Verlustwinkel im E<sub>010</sub>-Mikrowellenresonator," A.E.Ü., vol.20, no.9, pp.501–505, 1966.
- [3] T. Miura, T. Takahashi, and M. Kobayashi, "Accurate Q-factor evaluation by resonance curve area method and its application to the cavity perturbation," IEICE Trans. Electron., vol.E77-C, no.6, pp.900–907, June 1994.
- [4] A.J. Estlin and H.E. Bussey, "Errors in dielectric measurements due to a sample insertion hole in a cavity," IRE Trans. Microw. Theory Tech., vol.MTT-8, no.6, pp.650–653, Nov. 1960.
- [5] W. Meyer, "Dielectric measurements on polymeric materials by using superconducting microwave resonators," IEEE Trans. Microw. Theory Tech., vol.MTT-25, no.12, pp.1092–1099, Dec. 1977.
- [6] S.H. Li, C. Akyel, and R.G. Bosisio, "Precise calculations and measurements on the complex dielectric constant of lossy materials using TM<sub>010</sub> cavity perturbation techniques," IEEE Trans. Microw. Theory Tech., vol.MTT-29, no.10, pp.1041–1048, Oct. 1981.
- [7] S.H. Li and R.G. Bosisio, "Composite hole conditions on complex permittivity measurements using microwave cavity perturbation techniques," IEEE Trans. Microw. Theory Tech., vol.MTT-30, no.1, pp.100–103, Jan. 1982.
- [8] B.Y. Kapilevich, S.G. Ogourtsov, V.G. Belenky, A.B. Maslenikov, and A.S. Omar, "Accurate microwave resonant method for complex permittivity measurements of liquids," IEEE Trans. Microw. Theory Tech., vol.48, no.11, pp.2159–2164, Nov. 2000.
- [9] H. Kawabata, H. Tanpo, and Y. Kobayashi, "An improvement of the perturbation method using a TM<sub>010</sub> mode cylindrical cavity," IEICE Trans. Electron., vol.E86-C, no.12, pp.2371–2378, Dec. 2003.
- [10] H. Kawabata, H. Tanpo, and Y. Kobayashi, "A rigorous analysis of a TM<sub>010</sub> mode cylindrical cavity to measure accurate complex permittivity of liquid," 33rd European Microwave Conf., Munich, pp.759–762, Oct. 2003.
- [11] H. Kawabata, H. Tanpo, and Y. Kobayashi, "An improvement of perturbation method for the complex permittivity measurements of liquids," 2003 Asia-Pacific Microwave Conf., Seoul, WEP-65, pp.576–579, Nov. 2003.
- [12] Chemical Society of Japan, Kagaku benran (kisoheon 2), Maruzen, Tokyo, 1991.

## Appendix A: Derivation of Eq. (1)

The time factor  $e^{j\omega t}$  is neglected. The  $z$ -components of the electric Hertz vector in each region are given by

$$\Pi_{e1} = \sum_{p=0}^{M-1} A_p J_0(k_{r1p}r) \begin{Bmatrix} \cos(\beta_{1p}z) \\ \sin(\beta_{1p}z) \end{Bmatrix} \quad (\text{A} \cdot 1)$$

$$\Pi_{e2} = \sum_{p=0}^{M-1} \{B_{2p} J_0(k_{r2p}r) + C_{2p} Y_0(k_{r2p}r)\} \times \begin{Bmatrix} \cos(\beta_{2p}z) \\ \sin(\beta_{2p}z) \end{Bmatrix} \quad (\text{A} \cdot 2)$$

$$\Pi_{e3} = \sum_{p=0}^{M-1} \{B_{3p} J_0(k_{r3p}r) + C_{3p} Y_0(k_{r3p}r)\}$$

$$\times \begin{Bmatrix} \cos(\beta_{3p}z) \\ \sin(\beta_{3p}z) \end{Bmatrix} \quad (\text{A} \cdot 3)$$

$$\Pi_{e4} = \sum_{q=0}^{N-1} D_q G_0(k_{r4q}r) \begin{Bmatrix} \cos(\beta_{4q}z) \\ \sin(\beta_{4q}z) \end{Bmatrix} \quad (\text{A} \cdot 4)$$

where

$$G_n(x) = J_n(x) - \frac{J_0(k_{r4q}R_4)}{Y_0(k_{r4q}R_4)} Y_n(x) \quad (\text{A} \cdot 5)$$

$$k_{rip}^2 = \epsilon_{ri} k_0^2 - \beta_{ip}^2, \quad k_0 = \frac{\omega}{c_0}. \quad (\text{A} \cdot 6)$$

The upper and lower expressions in brackets in Eqs. (A·1)–(A·4) correspond to two cases of the electric or magnetic wall condition at  $z=0$ , respectively. Also,  $\beta$  is defined as follows ( $i=1,2,3$ ):

$$\beta_{ip} = \begin{Bmatrix} \frac{p}{H} \pi \\ p + \frac{1}{2} \pi \end{Bmatrix}, \quad \beta_{4q} = \frac{q}{L} \pi \quad (\text{A} \cdot 7)$$

for the electric wall condition at  $z = 0$  and

$$\beta_{ip} = \begin{Bmatrix} \frac{p + \frac{1}{2}}{H} \pi \\ \frac{p + 1}{H} \pi \end{Bmatrix}, \quad \beta_{4q} = \frac{q + \frac{1}{2}}{L} \pi \quad (\text{A} \cdot 8)$$

for the magnetic wall condition at  $z=0$ . Where the upper and lower expressions in Eqs. (A·7) and (A·8) correspond to two cases of the electric and magnetic wall condition at  $z = H$ , respectively.  $J_n(x)$  and  $Y_n(x)$  are the Bessel functions of the 1st and 2nd kind, respectively. The prime symbols (') indicate differentiation with respect to  $x$ .

The field components in each region are given by:

$$E_r = \frac{\partial^2 \Pi_e}{\partial r \partial z}, \quad E_z = \frac{\partial^2 \Pi_e}{\partial z^2} + \epsilon_r k_0^2 \Pi_e \quad (\text{A} \cdot 9)$$

$$H_\theta = -j\omega \epsilon_r \epsilon_0 \frac{\partial \Pi_e}{\partial r}. \quad (\text{A} \cdot 10)$$

Imposing the boundary conditions that  $E_r$  and  $H_\theta$  be continuous at  $r = R_1$  and  $R_2$ , the relationships among coefficients  $A_p$ ,  $B_{2p}$ ,  $C_{2p}$ ,  $B_{3p}$  and  $C_{3p}$  are obtained as follows:

$$\begin{bmatrix} \bar{B}_{2p} \\ \bar{C}_{2p} \end{bmatrix} = \begin{bmatrix} \frac{B_{2p}}{A_p} \\ \frac{C_{2p}}{A_p} \end{bmatrix} = \mathbf{D}_2^{-1} \mathbf{C}_1 \quad (\text{A} \cdot 11)$$

$$\begin{bmatrix} \bar{B}_{3p} \\ \bar{C}_{3p} \end{bmatrix} = \begin{bmatrix} \frac{B_{3p}}{A_p} \\ \frac{C_{3p}}{A_p} \end{bmatrix} = \mathbf{D}_3^{-1} \mathbf{C}_2 \begin{bmatrix} \bar{B}_{2p} \\ \bar{C}_{2p} \end{bmatrix} = \mathbf{D}_3^{-1} \mathbf{C}_2 \mathbf{D}_2^{-1} \mathbf{C}_1 \quad (\text{A} \cdot 12)$$

where

$$\mathbf{C}_1 = \begin{bmatrix} \frac{k_{r1p}^2}{k_{r2p}^2} J_0(k_{r1p}R_1) \\ \frac{\varepsilon_{r1}k_{r1p}}{\varepsilon_{r2}k_{r2p}} J'_0(k_{r1p}R_1) \end{bmatrix} \quad (\text{A} \cdot 13)$$

$$\mathbf{D}_2 = \begin{bmatrix} J_0(k_{r2p}R_1) & Y_0(k_{r2p}R_1) \\ J'_0(k_{r2p}R_1) & Y'_0(k_{r2p}R_1) \end{bmatrix} \quad (\text{A} \cdot 14)$$

$$\mathbf{C}_2 = \begin{bmatrix} \frac{k_{r2p}^2}{k_{r3p}^2} J_0(k_{r2p}R_2) & \frac{k_{r2p}^2}{k_{r3p}^2} Y_0(k_{r2p}R_2) \\ \frac{\varepsilon_{r2}k_{r2p}}{\varepsilon_{r3}k_{r3p}} J'_0(k_{r2p}R_2) & \frac{\varepsilon_{r2}k_{r2p}}{\varepsilon_{r3}k_{r3p}} Y'_0(k_{r2p}R_2) \end{bmatrix} \quad (\text{A} \cdot 15)$$

$$\mathbf{D}_3 = \begin{bmatrix} J_0(k_{r3p}R_2) & Y_0(k_{r3p}R_2) \\ J'_0(k_{r3p}R_2) & Y'_0(k_{r3p}R_2) \end{bmatrix}. \quad (\text{A} \cdot 16)$$

$\mathbf{D}_2^{-1}$  and  $\mathbf{D}_3^{-1}$  mean the inverse matrices of  $\mathbf{D}_2$  and  $\mathbf{D}_3$ , respectively.

In a similar way to the case of a dielectric rods [9], the unknown  $z$ -component of electric field  $E_{bd}(z)$  is defined on the boundary between the region 3 and 4 ( $r = R_3$ ).

$$E_{bd}(z) = \sum_{p=0}^{M-1} A_p k_{r3p}^2 \left\{ \bar{B}_{3p} J_0(k_{r3p}R_3) + \bar{C}_{3p} Y_0(k_{r3p}R_3) \right\} \begin{Bmatrix} \cos(\beta_{3p}z) \\ \sin(\beta_{3p}z) \end{Bmatrix} \quad (\text{A} \cdot 17)$$

$$= \sum_{q=0}^{N-1} D_q k_{r4q}^2 G_0(k_{r4q}R_3) \begin{Bmatrix} \cos(\beta_{4q}z) \\ \sin(\beta_{4q}z) \end{Bmatrix}. \quad (\text{A} \cdot 18)$$

$A_p$  and  $D_q$  are related to  $E_{bd}(z)$  by using the orthogonality of the trigonometric functions. From the boundary condition of  $H_\theta(z)$  at  $r = R_3$ , the following integral equation is obtained:

$$\sum_{p=0}^{M-1} \frac{\varepsilon_{r3}}{\eta_p H} H_p P_{pq} \int_0^H E_{bd}(z) \begin{Bmatrix} \cos(\beta_{3p}z) \\ \sin(\beta_{3p}z) \end{Bmatrix} dz = \frac{\varepsilon_{r4}}{L} S_q \int_0^L E_{bd}(z) \begin{Bmatrix} \cos(\beta_{4q}z) \\ \sin(\beta_{4q}z) \end{Bmatrix} dz \quad (\text{A} \cdot 19)$$

where

$$H_p = \frac{k_{r3p}}{k_{r3p}^2 R_3} \times \frac{\bar{B}_{3p} J'_0(k_{r3p}R_3) + \bar{C}_{3p} Y'_0(k_{r3p}R_3)}{\bar{B}_{3p} J_0(k_{r3p}R_3) + \bar{C}_{3p} Y_0(k_{r3p}R_3)} \quad (\text{A} \cdot 20)$$

$$S_q = \frac{k_{r4q}}{k_{r4q}^2 R_3} \frac{G'_0(k_{r4q}R_3)}{G_0(k_{r4q}R_3)} \quad (\text{A} \cdot 21)$$

$$P_{pq} = \begin{cases} + \\ - \end{cases} \frac{\sin\{(\beta_{3p} + \beta_{4q})L\}}{(\beta_{3p} + \beta_{4q})L} + \frac{\sin\{(\beta_{3p} - \beta_{4q})L\}}{(\beta_{3p} - \beta_{4q})L}. \quad (\text{A} \cdot 22)$$

To solve Eq.(A·19) by the Ritz-Galerkin Method,  $E_{bd}(z)$  is put into the following form:

$$E_{bd}(z) = \begin{cases} E_{3z}(z) = E_{4z}(z) : & 0 \leq z \leq L \\ 0 : & L \leq z \leq H \end{cases} \quad (\text{A} \cdot 23)$$

where

$$E_{4z}(z) = \sum_{l=0}^{N-1} E_l \begin{Bmatrix} \cos(\beta_{4l}z) \\ \sin(\beta_{4l}z) \end{Bmatrix}. \quad (\text{A} \cdot 24)$$

Thus, the following homogeneous equations for the expansion coefficients  $E_l$  are obtained:

$$[X_{ql}] [E_l] = [0] \quad (\text{A} \cdot 25)$$

where

$$X_{ql} = \delta_{ql} \varepsilon_{r4} \begin{Bmatrix} \eta_q \\ 1 \end{Bmatrix} S_q - \varepsilon_{r3} \frac{L}{H} \sum_{p=0}^{M-1} \frac{1}{\begin{Bmatrix} \eta_p \\ 1 \end{Bmatrix}} P_{pq} P_{pl}. \quad (\text{A} \cdot 26)$$

Furthermore,

$$\delta_{ql} = \begin{cases} 1 : & q = l \\ 0 : & q \neq l \end{cases} \quad (\text{A} \cdot 27)$$

$$\eta_p = \begin{cases} 2 : & \beta_{3p} = 0 \\ 1 : & \beta_{3p} \neq 0 \end{cases}. \quad (\text{A} \cdot 28)$$

## Appendix B: Expansion Coefficients

When the nontrivial solution of Eq. (A·25) is obtained, the values of  $E_l$  can be determined. At first,  $A_p$  and  $D_q$  can be calculated by using Eq. (A·17) and (A·18), respectively, as follows:

$$A_p = \frac{L}{\begin{Bmatrix} \eta_p \\ 1 \end{Bmatrix} H k_{r3p}^2} \sum_{l=0}^{N-1} E_l P_{pl} \times \frac{\bar{B}_{3p} J_0(k_{r3p}R_3) + \bar{C}_{3p} Y_0(k_{r3p}R_3)}{E_q} \quad (\text{A} \cdot 29)$$

$$D_q = \frac{E_q}{k_{r4q}^2 G_0(k_{r4q}R_3)}. \quad (\text{A} \cdot 30)$$

Then,  $B_{2p}$ ,  $C_{2p}$ ,  $B_{3p}$  and  $C_{3p}$  are obtained from Eqs. (A·29), (A·11) and (A·12).



**Hirokazu Kawabata** was born in Gumma, Japan, in July 1959. He received the B.E. and M.E. degrees in electrical engineering from University of Electro-Communications, Tokyo, Japan, in 1983 and 1985, respectively. He is presently interested in measurements of complex permittivity of dielectric materials. He is a member of the Institute of Electrical and Electronics Engineers.



**Hiroshi Tanpo** was born in Toyama, Japan, in February 1979. He received the B.E. and M.E. degrees in electrical engineering from Saitama University, Japan, in 2001 and 2003, respectively. He has engaged in research for measurements of complex permittivity of dielectric materials.



**Yoshio Kobayashi** was born in Japan on July 4, 1939. He received the B.E., M.E., and D.Eng. degrees in electrical engineering from Tokyo Metropolitan University, Tokyo, Japan, in 1963, 1965, and 1982, respectively. Since 1965, he has been with Saitama University, Saitama, Japan. He is now a professor at the same university. His current research interests are in dielectric resonators and filters, measurements of low-loss dielectric and high-temperature superconductive (HTS) materials, and HTS filters,

in microwave and millimeter wave region. He served as the Chair of the Technical Group on Microwaves, IEICE, from 1993 to 1994, as the Chair of the Technical Group of Microwave Simulators, IEICE, from 1995 to 1997, as the Chair of Technical Committee on Millimeter-wave Communications and Sensing, IEE Japan, from 1993 to 1995, as the Chair of Steering Committee, 1998 Asia Pacific Microwave Conference (APMC'98) held in Yokohama, as the Chair of the National Committee of APMC, IEICE from 1999 to 2000, and as the Chair of the IEEE MTT-S Tokyo Chapter from 1995 to 1996. He also serves as a member of the National Committee of IEC TC49 since 1991, the Chair of the National Committee of IEC TC49 WG10 since 1999 and a member of the National Committee of IEC TC90 WG8 since 1997. Prof. Kobayashi received the Inoue Harushige Award on "Dielectric filters for mobile communication base stations" in 1995. He is a Fellow of IEEE.